Material defects: the variational modeling and analysis of dislocations

Adriana Garroni

PhD Course - GSSI 2015

Contents

Chapter 1

Introduction to dislocations

The focus on the course will be the analysis of variational models for dislocations. These are topological defects in crystals that represent the main mechanism for their plastic behavior. There is a large mechanical, numerical and theoretical literature about dislocations, but many important questions are still open. The mathematical understanding of these objects and related models, on one hand give rise to very interesting and deep mathematical issues, on the other hand can provide an improvement of the existing models to explain some of the unexplored phenomena related with dislocations.

1.1 A phenomenological description

We start this course with a quick and schematic phenomenological description of dislocations and their role in plastic behavior.

1.1.1 Elastic vs Plastic

The first step is to identify the difference between elastic and plastic deformation. These are familiar notions and it is easy to understand the core of the matter by means of a very simple one-dimension ideal experiment. We consider a bar (say of metal) and we stretch it. It behaves elastically if the corresponding elongation is approximatively proportional to the internal stress and that, once we release the load, the bar goes back to its original configuration (as illustrated in the Figure 1.1 a)). In other words an elastic deformation is completely reversible and after a loading cycle the final configuration is the same as the initial one.

Now, increasing the load over a given critical stress (the yielding stress $\sigma_{critical}$), the bar becomes softer (phase 2 in Figure 1.1 b)), and in the unloading process the deformation follows a different path (phase 3 in Figure 1.1 b)) ending with a permanent deformation, a *plastic deformation.*

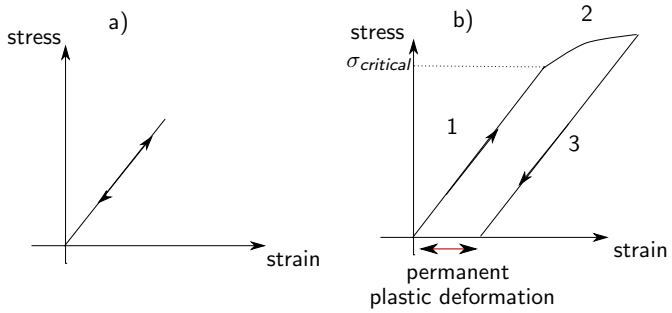

Figure 1.1: a) Shows a schematic loading cycle with an elastic response; b) Corresponds to a cycles for an elasto-plastic response ending with a permanent plastic deformation.

We can understand which is the mechanism for plastic deformation in metals, again with an idealized experiment. Note that many materials exhibit plastic behavior and the reasons, although similar, might depend on the "microscopic" structure of the material. Metals are crystals, i.e. they are characterized by a regular distribution of atoms that lie on a lattice. We will then focus on crystal plasticity. We will also study some of the most common crystalline structures in metal, but for the sake of simplicity we will describe the plastic mechanism using a two dimensional cartoon which represents a domain with an underlying square lattice subject to a load.

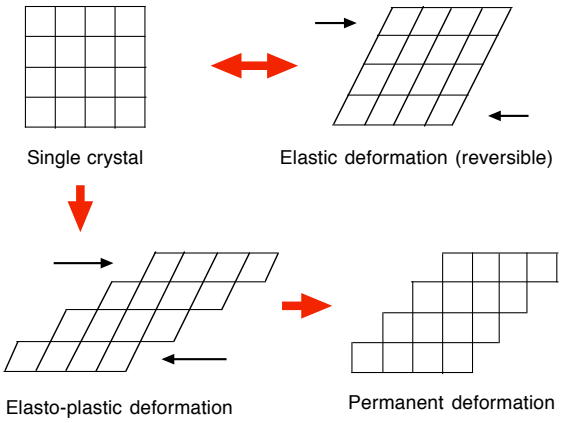

Figure 1.2: Comparison between elastic and plastic deformation in a crystalline structure

The picture in Figure 1.2 at the top on the left represents the crystal at the equilibrium, the reference configuration (we suppose that without

external load the atoms have minimal interaction energy in the square lattice). Applying a load, we observe a shear resulting in a distortion of the lattice (a small deviation from the reference configuration). Releasing the load the deformation is completely reversible (represented by the double arrow in Figure 1.2); this is an elastic deformation. If now we increase the load we observe sliding along horizontal lines (bottom of Figure 1.2). This is an elasto-plastic deformation. Unloading we then obtain that the elastic distortion is released but we end up with a permanent deformation.

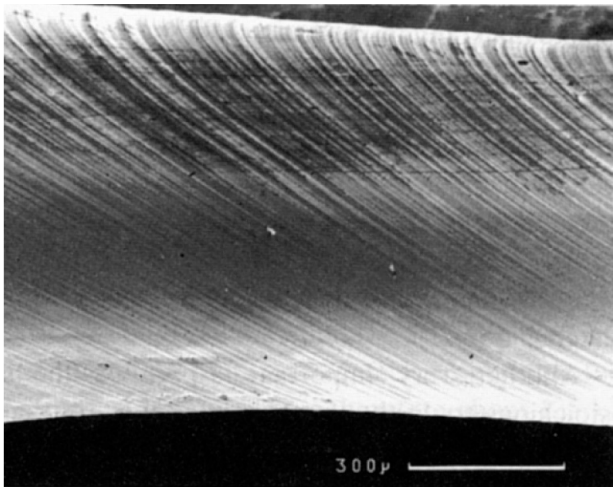

Figure 1.3: http://www.doitpoms.ac.uk/tlplib/slip/index.php

This mechanism for deformation of metals was already observed in the nineteen century with optical micrographs, even thought the crystalline nature of metals was not yet understood. At the beginning of last century the importance of slips for plastic deformation was recognized and scientists were studing the elastic behavior of bodies subject to different types of deformations related with slips. The most relevant contribution was that of Vito Volterra (1907) who computed explicitly the strain and stress fields for the deformation for the cylinders with cuts illustrated in Figure 1.4 Several macroscopic (continuum) models for (crystal) plasticity are still based on this idea.

1.1.2 The idea of dislocations

The mechanism described above for plastic deformation was not able to explain some relevant issues arising from experiments. The main open question was how to explain the discrepancy between the theoretical yielding stress and the measured one. Indeed, in the 1930s the micrographs were

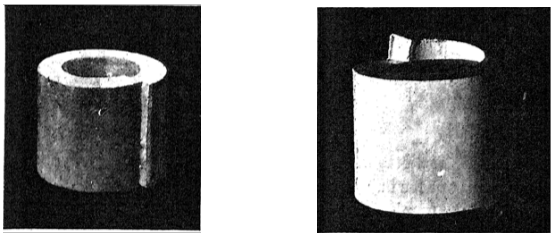

Figure 1.4: V. Volterra, **Sur l'équilibre des corps élastiques multiplement connexes** Annales scient. de l'E.N.S. tome 24 (1907)

strong enough to permit to discover the crystallographic nature of the metals. Based on this new knowledge it was possible to estimate a theoretical yielding threshold that tuned out to be orders of magnitude larger than the measured yielding threshold (i.e. the critical stress $\sigma_{critical}$ at which plastic flow actually starts). The theoretical threshold was obtained via an *ab initio* calculation based on the idea that in order to start gliding atoms should overcome an energy barrier due to the interaction with the neighboring atoms. The height of this energy barriers is proportional to the theoretical stress threshold, σ_{th}[1].

Another important point is the presence of hardening phenomena. In fact after several cycles of loading and unloading in different directions the material experiences *hardening* (i.e., an increase of the resistance of the material to undergo plastic flow). These and other effects cannot be explained by this simple slipping mechanism.

It was in order to explain this discrepancy that, in 1934, the presence of dislocations was first conjectured by Orowan, Polanyi, and Taylor, the idea behind this conjecture being that this slipping mechanism could also be related to the presence of crystal defects.

At a discrete level a dislocation is represented (for the simple, yet unre-

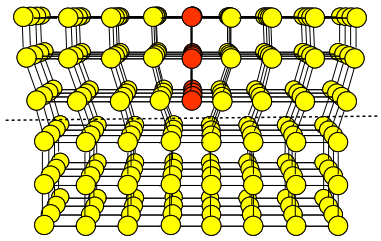

Figure 1.5: The upper part of the crystal has an extra plane of atoms and the edge of this plane is the region in which the defected crystal cannot be matched with a perfect cubic crystal (this line is a so called *dislocation*)

alistic cubic crystal) in Figure 1.5.

These defects are strictly related with the gliding mechanism. In general, during plastic flow, the slip is not uniform and this is related with the presence and the formation of dislocations. This concept is clarified by the following definition of dislocations *à la Volterra* (inspired by the elastic solutions of Volterra for cylinders with cuts that we have already mentioned): *dislocations can be understood as lines separating regions that underwent different slips.*

[1] In a first approximation (Frenkel 1926) the elastic stress on each atom, due to the interaction with other atoms, when it deviates by x from its equilibrium configuration is of the form

$$\sigma = \sigma_{th} \sin \frac{2\pi x}{b}$$

where b is the interatomic distance, while for small shears one has

$$\sigma = \mu \frac{x}{d}$$

where μ is the shear modulus and d the interplanar distance. These two representations are at the basis of the estimate of the theoretical yield stress. Indeed in the small strain limit we have $\sin(2\pi x/b) \sim 2\pi x/b$, which gives

$$\sigma_{th} \sim \frac{\mu b}{2\pi d}$$

(see [8], Chapter 1).

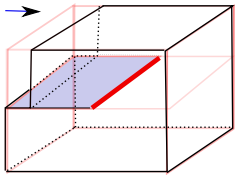

Figure 1.6: The red line represents an edge dislocation

This description makes it clear that ideally dislocations are lines. The dislocation described in Figure 1.6 is called an *edge dislocation*, as well as the one depicted at a discrete level in Figure 1.5. A classical way to detect dislocations at a discrete level is represented in Figure 1.7.

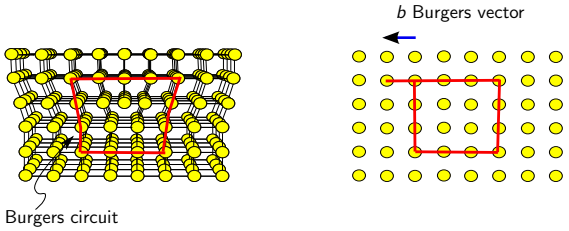

Figure 1.7: The definition of the Burgers vector through the Burgers circuit

The procedure (suggested by Frank, 1951) consists in drawing a circuit around the dislocation in the defected crystal. As you can observe the region outside the circuit is locally a small deformation of a perfect crystal while the region inside (the *core region*) contains the defect. If we now draw the same circuit in a reference configuration (with a perfect crystal) we can see that, whenever inside the first circuit there is a defect, the circuit in the perfect crystal does not close. The missing vector represents the *strength* of the dislocation and is called the *Burgers vector* of the dislocation. An edge dislocation is then a straight line equipped with a Burgers vector orthogonal to the line. From the picture it is clear that the Burgers vector does not depend on the choice of the circuit, as far as the circuit contains only one defect. We will see later that in fact the Burgers vector is a topological invariant and, in this respect, dislocations can be considered a topological defects.

There is another important class of dislocations, *screw dislocations*. These are characterize by a Burgers vector parallel to the line, and they may be obtained kinematically *à la Volterra* with a slip parallel to the line, as illustrated in Figure 1.8. In general a dislocation line might be neither edge nor screw, but at a microscopic scale can be understood as made of infinitesimal edge and screw dislocations. Why dislocations are so important and why

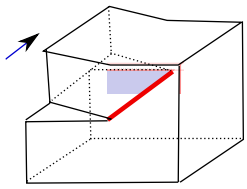

Figure 1.8: The red line represents a screw dislocation

they are the answer to the questions the we raised above? The reason is that their motion favors the plastic slip.

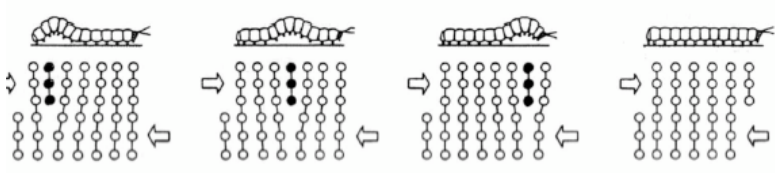

Figure 1.9: Motion of dislocations as a mechanism for plastic slip (Lloyd, Molina-Aldareguia 2003)

Figure 1.10: The example of the carpet highlight the one dimensional nature of these defects (Cacace 2004)

In Figures 1.9 and 1.10 you can find to classical examples used to explain the effect of defects (moving a bump for the caterpillar produces a final displacement with less effort, than jumping all at once, as well as pushing a crease of the heavy carpet is easier than moving the whole carpet at the same time). The example of the carpet is also interesting since it makes clear that since this gliding mechanism occurs on a plane (the floor) the defect (the crease) should be necessary a line.

Note that dislocations were conjectured based on this mechanism, much

earlier than being observed. The first observations at a Transmission Electron Micrograph was possible only starting from the 1950s.

A last very important ingredient in the understanding of dislocations is the *crystallographic structure*.

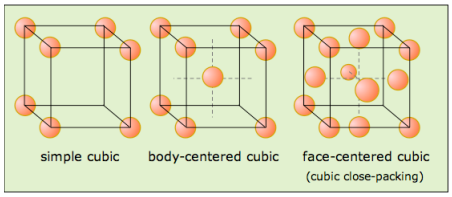

Figure 1.11: http://chemwiki.ucdavis.edu/

Indeed dislocations in general belong to a class of admissible planes and may admit as Burgers vectors a given class of vectors, so that the a slip along that plane by the Burgers vector represents a transformation under which the underlying lattice is invariant. In general the *slip plane* is determined by the two vectors $\mathbf{b}$ and $\mathbf{t}$, the Burgers vector and the direction of the dislocation line. The only case in which the slip plane is not uniquely determined, but depends on the crystal under consideration, is the case of screw dislocations (for which $\mathbf{b}$ and $\mathbf{t}$ are parallel). The pairs of admissible planes and corresponding admissible Burgers vectors are called *slip systems*. Slip systems are important for the understanding of the interaction and the motion of dislocations. For the sake of simplicity in most of these notes we will consider only the case of the cubic lattice, which is not realistic. Nevertheless this analysis is enough in order to understand the fundamental facts, being the most relevant crystallographic structure for metals, *Body Center Cubic (BCC)* and *Face Center Cubic (FCC)* lattices (Figure 1.11), both with cubic symmetry.

These two structures present 12 slip systems, some of them illustrated in Figure 1.12 (for some details about the specific properties of dislocations in different crystalline structure see e.g. [9]).

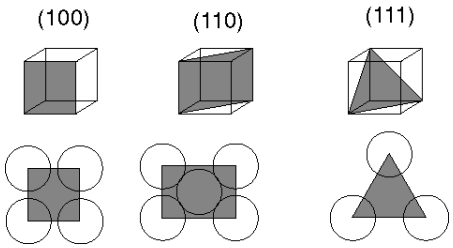

Figure 1.12

The crystallographic structure in clearly very relevant to understanding the interaction of dislocations, their kinematic constraints and their motion. Effective continuum models for plasticity should then account for the anisotropic effects due to the crystallographic details of the underlying crystal. Many intermediate scales are relevant in the study of crystal plasticity (see Figure 1.13).

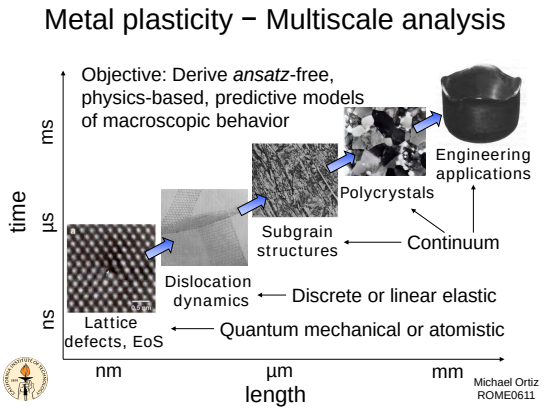

Figure 1.13: One of the slides of course of M. Ortiz, Rome 2011

The final goal of our analysis is to bridge the scales, with a multi-scale (ansatz free) analysis, improving existing continuum models with informations coming from a discrete (atomistic) description.

1.2 A quick review of the elastic continuum theory for dislocations

1.2.1 Kinematics

In the theory of elasticity on can represent a deformation of a body using a reference configuration $\Omega \subset \mathbb{R}^3$ and a function $v : \Omega \to \mathbb{R}^3$

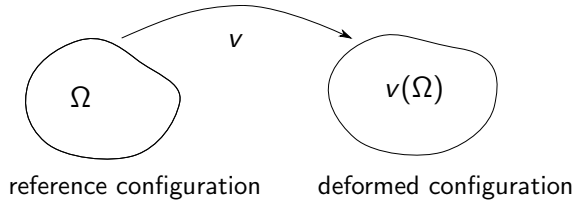

Figure 1.14: Deformation of a body

Assuming that the reference configuration is the body at equilibrium, it is also convenient to measure the deformation using the deviation from the identity, which correspond to use as a relevant variable the *displacement*, i.e. a function $u : \Omega \to \mathbb{R}^3$ such that

$$v(x) = x + u(x)\,.$$

We now include the possibility of plastic slips during deformation. We fix a regular (e.g. Lipschitz, with Lipschitz boundary γ) surface Σ in Ω and we assume that

1. u is regular outside the surface Σ, e.g. $u \in W^{1,1}(\Omega \setminus \Sigma, \mathbb{R}^3)$;
2. u has a discontinuity across Σ;
3. the jump of u, $[u] := u^+ - u^-$ with u^+ and u^- the two traces of u on the two sides of Σ, is parallel to Σ. In other words we require that $[u] \cdot n = 0$, with n the normal to the surface Σ.

A functional space in which these requirements are well posed in a proper weak sense is the space $SBV(\Omega; \mathbb{R}^3)$ (of the Special Functions with Bounded Variation - see [6, 2]). We will come back to this technical point later on. For the moment the above condition are enough to describe the main ingredients of the kinematic. If we now compute the distributional gradient of u we obtain that

$$Du = \nabla u \mathcal{L}^3 + [u] \otimes n \mathcal{H}^2 \llcorner \Sigma\,, \tag{1.2.1}$$

where $\mathcal{L}^3$ denotes the 3-dimensional Lebesgue measure, while $\mathcal{H}^2 \llcorner \Sigma$ is the 2-dimensional Hausdorff measure on Σ (see e.g. [6]), which in this regular

case reduces to the classical surface measure on Σ. The expression (1.2.1) for the distributional gradient of u is an example of a more general situation occurring in the linear theory for plasticity, where the deformation gradient is decomposed in an elastic strain β^e and a plastic strain β^p, i.e.

$$Du = \beta^e + \beta^p \,, \tag{1.2.2}$$

In (1.2.1) $\nabla u \mathcal{L}^3 =: \beta^e$ is absolutely continuous with respect to the 3-dimensional Lebesgue measure and can be interpreted as the elastic bulk distortion, while $[u] \otimes n\mathcal{H}^2 \llcorner \Sigma =: \beta^p$ is the plastic deformation due to slips. Note that in the classical elasto-plastic models (see e.g. [11]) the decomposition (1.2.2) is done at a macroscopic scale in which the effective plastic deformation is understood as the result of many slips that occurs at smaller scales, so it need not to be an actual slip, and hence is not necessary concentrated on surfaces (see e.g. [4]).

Since Du is a gradient we have that the distributional curl of Du is zero,

$$\mathrm{Curl} Du = 0 \quad \text{in the sense of distributions in } \Omega \tag{1.2.3}$$

(here we are denoting by $\mathrm{Curl}\beta$ the curl of a 3×3 matrix β, which corresponds to the a matrix whose rows are the curl of the rows of β)[2]. Hence we have that

$$\mathrm{Curl}\beta^e = -\mathrm{Curl}\beta^p \,.$$

We also want to include the ingredient that the slips should be compatible with the underlying lattice (at least locally). This corresponds to require that the jump of u belongs to the set of *admissible Burgers vectors* that we will denote by $\mathcal{B}$, which in the case of the cubic lattice coincides with $\mathbb{Z}^3$. From (1.2.3), taking $\Phi \in C_0^\infty(\Omega, \mathbb{R}^{3\times 3})$ and integrating by parts (using Stokes formula), we get

$$\langle \mathrm{Curl}\, \beta^e, \Phi \rangle := \int_\Omega \mathrm{Curl}\, \Phi \cdot \beta^e = \int_\Sigma \mathrm{Curl}\, \Phi [u] \otimes n d\mathcal{H}^2 \tag{1.2.4}$$

Now, if the slip is uniform, then there are no dislocations. This means that Σ disconnects Ω (or $\partial\Sigma \cap \Omega = \emptyset$) and $[u]$ must be constant on each connected component of Σ, hence by (1.2.4) we get

$$\langle \mathrm{Curl}\, \beta^e, \Phi \rangle = \int_{\partial\Sigma\cap\Omega} \Phi[u] \otimes t d\mathcal{H}^1 = 0$$

(where t is the tangent to $\partial\Sigma$) which implies, if Ω is simply connected, that β^e is a gradient in whole of Ω (i.e. there exists a function $v \in W^{1,1}(\Omega)$ such that $\nabla v = \beta^e$).

[2] $(\mathrm{Curl}\beta)_{ij} = \sum_{kl} e_{klj}\partial_k \beta_{il}$, with $e_{123} = 1 = e_{312} = e_{231}$ and $e_{321} = -1$

If, instead, we have non uniform slips we obtain that

$$\mathrm{Curl}\beta^e \neq 0\,.$$

We now apply the above formulas to the specific examples illustrated before.

For the edge dislocation in Figure 1.6 we take $\Sigma = \{x_3 = 0, x_2 < 0\}$ so that the dislocation line γ is given by $\gamma = e_1\mathbb{R}$, where e_1, e_2, e_3 denotes the canonical basis in $\mathbb{R}^3$. We choose $u \in W^{1,1}(\Omega \setminus \Sigma)$ with

$$[u] = \begin{cases} be_2 & x = (x_1, x_2, 0) \text{ with } x_2 < 0 \\ 0 & \text{otherwise} \end{cases} \tag{1.2.5}$$

where $b \in \mathbb{Z}$ and $\mathbf{b} = be_2$ is the Burgers vector[3].

For the screw dislocation in Figure 1.8 again we take $\Sigma = \{x_3 = 0, x_2 < 0\}$ and $\gamma = e_1\mathbb{R}$, and we choose $u \in W^{1,1}(\Omega \setminus \Sigma)$ with

$$[u] = \begin{cases} -be_1 & x = (x_1, x_2, 0) \text{ with } x_2 < 0 \\ 0 & \text{otherwise} \end{cases} \tag{1.2.6}$$

with $b \in \mathbb{Z}$ and $\mathbf{b} = -be_1$ is the Burgers vector.

Finally for an arbitrary loop in the plane $\{x_3 = 0\}$ as in Figure 1.15 we

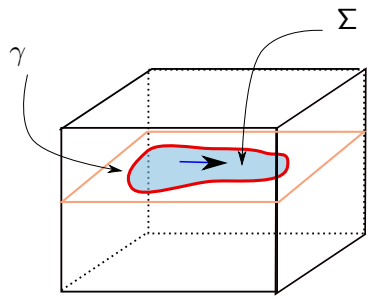

Figure 1.15: The slip that produces a loop on Σ

take

$$[u] = \begin{cases} \mathbf{b} & x \in \Sigma \\ 0 & \text{otherwise}\,. \end{cases} \tag{1.2.7}$$

In all these cases we obtain

$$\mathrm{Curl}\beta^e = \mathrm{Curl}\,\nabla u = \mathbf{b} \otimes \frac{\gamma'}{|\gamma'|}\mathcal{H}^1 \llcorner \gamma \qquad \text{in } \Omega\,, \tag{1.2.8}$$

[3]The fact that it is possible to find a function with this regularity satisfying (1.2.5) ((1.2.6), or (1.2.7)) will be discussed later

where with an abuse of notation we are using γ to denote the close curve and its parametrization, so that $\frac{\gamma'}{|\gamma'|}$ is the tangent to γ, while $\mathcal{H}^1 \llcorner \gamma$ is the 1-dimensional Hausdorff measure on γ, which if γ is a Lipschitz curve, coincides with the line measure on γ.

The examples above are consistent with the Volterra description of dislocations and provide a continuum version of the Burgers circuit that we have introduced at a discrete level. Indeed from (1.2.8) we obtain that for every circuit C around γ[4], as in Figure 1.16, we have that the circulation of β^e around C is given by $\mathbf{b}$, i.e.,

$$\int_C \beta^e \cdot \tau = \mathbf{b}\,, \tag{1.2.9}$$

where τ is the tangent to C. This formula clarify the fact that dislocations are topological defects of the elastic strain field.

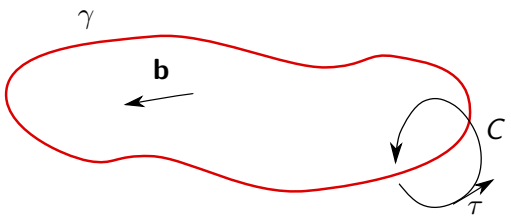

Figure 1.16: The circulation around a circuit

The matrix-valued measure $\mu = \mathbf{b} \otimes \frac{\gamma'}{|\gamma'|} \mathcal{H}^1 \llcorner \gamma$ is called the *Nye dislocation measure* corresponding to the strain β^e.

In general, as we already mentioned, in the context of the linear macroscopic theory for plasticity the decomposition in plastic and elastic strain does not requires the structure given in (1.2.2), nevertheless we can interpret the condition $\operatorname{Curl} \beta^e \neq 0$ as a consequence of the presence of dislocations at a smaller scale. In the literature the quantity

$$\alpha := \operatorname{Curl} \beta^e$$

is called the *Nye dislocation density* [12]. By its very definition, we have that α should satisfy

$$\operatorname{Div} \alpha = 0 \quad \text{in the sense of distributions in } \Omega\,,^5 \tag{1.2.10}$$

or equivalently

$$\int_\Omega D\Phi \cdot \alpha = 0 \qquad \forall \Phi \in C_0^\infty(\Omega)\,.$$

[4]Precisely we should require that C is closed curve, which is the boundary of a surface that intersect γ in one point

In particular in the case of a dislocation line γ, i.e. $\alpha = \mu = \mathbf{b} \otimes t\mathcal{H}^1 \llcorner \gamma$, this means that γ must be the union of a countable number of Lipschitz curves with no end-points in Ω, $\mathbf{b}$ must be constant on each connected component of γ away from branching points, and in each branching point the oriented sum of Burgers vectors must be zero (see Figure 1.17).

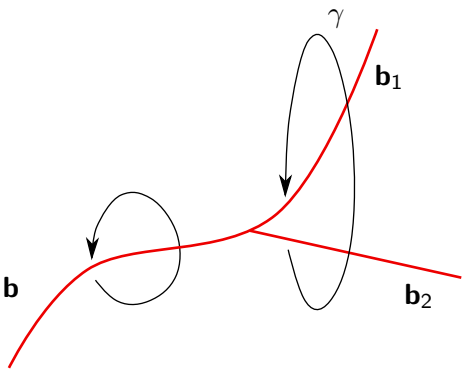

Figure 1.17: Burgers vectors at branching points. The Burgers circulation is a topological invariant, and hence $\mathbf{b} = \mathbf{b}_1 + \mathbf{b}_2$.

1.2.2 Elasticity

Before describing elastic properties of dislocations and their consequences in the continuum theories (see Section 1.2.3), we now give a very quick review of the essential notions in linear elasticity that will be required (see e.g. [7], [10] of [3] for a more complete treatment of elasticity theory).

A deformed elastic body is in a state of tension. In elasticity theory, using Cauchy stress principle, the internal forces present in the body are described by a stress tensor that represents the contact forces per unit area between two different parts of the body separated by an ideal surface. Then at each point of a reference configuration $\Omega \subset \mathbb{R}^3$ we define the stress tensor $\sigma \in \mathbb{R}^{3\times 3}$ (the Piola-Kirchoff stress tensor), where each component σ_{ij} represent i-th component of the contact force per unit area on a surface orthogonal to e_j (as illustrated in Figure 1.18).

The six components with $i \neq j$ are the shear stresses and using the balance of momentum one can show that $\sigma_{ij} = \sigma_{ji}$, i.e. σ is a symmetric tensor.

A theory, in elasticity, then corresponds to give a *constitutive relation* for the stress in terms of the deformation, i.e. to give an explicit dependence of σ in terms of the deformation v; this correspond to a condition on the material under consideration.

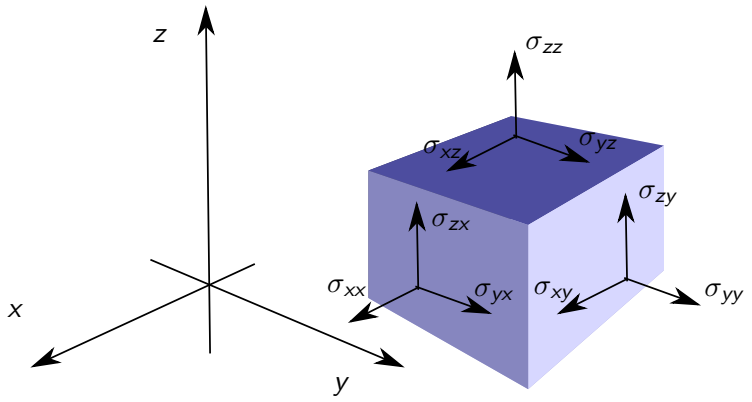

Figure 1.18

The first assumption that we always make, which can be obtained as a consequence of the thermodynamical axiom of positive work on closed baths (see [7], Section 28), is the property of *hyperelasticity*. We say the a material is *hyperelastic* if there exists a scalar function $W : \mathbb{R}^{3\times 3} \to \mathbb{R}$ such that[6]

$$\sigma_{ij}(F) = \frac{\partial W}{\partial F_{ij}}(F) \qquad \forall F \in \mathbb{R}^{3\times 3}\,. \tag{1.2.11}$$

This in particular implies that to an elastic deformation $v : \Omega \to \mathbb{R}^3$ we can associate an elastic energy given by

$$\int_\Omega W(\nabla v)\, dx\,. \tag{1.2.12}$$

We also assume that the reference configuration is the equilibrium at which we associate zero energy. This is expressed by

$$W(I) = 0 \qquad \text{and} \quad \frac{\partial W}{\partial F_{ij}}(I) = 0 \tag{1.2.13}$$

The assumption that the energy (1.2.12) be *frame indifferent*, which corresponds to the fact that the energy must be independent on the system of coordinates in which we represnts the deformed configuration and translate in terms of the energy density W in the following property

$$W(RF) = W(F) \qquad \forall F \in \mathbb{R}^{3\times 3} \text{ and } \forall R \in SO(3)\,. \tag{1.2.14}$$

Finally, as a consequence of frame indifference we can assume that W is a function of F^TF. Indeed for any given $F \in \mathbb{R}^{3\times 3}$, we can use the polar

[6] We consider only the *homogeneous* case, which correspond to the fact that $W(F)$ does not depend on $x \in \Omega$.

decomposition of F, and write

$$F = RU$$

for some rotation $R \in SO(3)$ and some symmetric matrix $U \in \mathbb{R}^{3\times 3}$, which then satisfies $U = \sqrt{F^T F}$. Together with (1.2.14) this implies that

$$W(F) = W(R^T F) = W(U) = W(\sqrt{F^T F}) = V(F^T F)\,. \tag{1.2.15}$$

From this general elastic energy, in a small displacement regime, i.e., assuming that $v(x) = x + \delta u(x)$ with δ small, we have

$$(I + \delta\nabla u)^T (I + \delta\nabla u) = I + \delta(\nabla u + \nabla u^T) + \delta^2 \nabla u^T \nabla u\,. \tag{1.2.16}$$

We can formally linearize the elastic energy[7] next to the identity (assuming enough regularity for the function W) and, using (1.2.15) and (1.2.16), we obtain

$$\int_\Omega W(I + \delta\nabla u)\,dx = \delta^2 \int_\Omega Ae(u)e(u)\,dx + o(\delta^2)\,,$$

where the elastic tensor A satisfies

$$A_{ijkl} = \frac{\partial^2 W}{\partial F_{ij}\partial F_{lk}}(I)\,,$$

and

$$e(u) = \frac{1}{2}(\nabla u + \nabla u^T)$$

is the *symmetrized gradient* of u. Exploiting the symmetries[8] of the tensor A we can introduce a symmetric matrix $\mathbb{C} \in \mathbb{R}^{3\times 3}$ which represents the *linearized elastic coefficients* satisfying the ellipticity condition

$$\mathbb{C}FF \geq c|F + F^T|^2\,, \qquad \text{with } c > 0 \qquad \forall F \in \mathbb{R}^{3\times 3}\,, \tag{1.2.17}$$

and the *linearized elastic energy* given by

$$\int_\Omega \mathbb{C}e(u) : e(u)\,dx\,, \tag{1.2.18}$$

here $G : F$ denotes the scalar product between matrices.

A further simplification of the elastic energy is obtained when the material is *isotropic* (i.e., it is invariant by rotations of the reference configuration). In this case the energy (1.2.18) reduces to the *isotropic linearized elastic energy*

$$\int_\Omega \frac{\lambda}{2}|\mathrm{tr}e(u)|^2 + \mu|e(u)|^2\,dx \tag{1.2.19}$$

where λ and μ are the *Lamè constants*.

[7] This formal linearization can also be obtained rigorously in terms of Γ-convergence (see [5])

[8] $A_{ijkl} = A_{klij} = A_{jikl}$

Exercise 1.2.1. *Given a triangolar two-dimensional lattice $\mathcal{L}$, as in Figure 1.19, generated by the vectors $v_1 = (1, 0)$ and $v_2 = (\frac{1}{2}, \frac{\sqrt{3}}{2})$ consider the points of the scaled lattice $\varepsilon\mathcal{L}$ as atoms connected by harmonic springs, and the following interaction energy*

$$\sum_{i,j\in\mathcal{L}\,:|i-j|=1} \varepsilon^2 \left(1 - \frac{|v_i - v_j|}{\varepsilon}\right)^2 ,$$

where $v : \varepsilon\mathcal{L} \to \mathbb{R}^2$ is the deformation of the lattice.

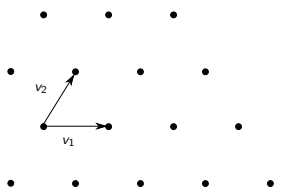

Figure 1.19

Now rewrite the energy in terms of a displacement $u : \varepsilon\mathcal{L} \to \mathbb{R}^2$ such that $v_i = \varepsilon i + \delta_\varepsilon u_i$ for $\delta_\varepsilon \ll \varepsilon$. Compute the limit as $\varepsilon \to 0$ of the energy

$$F_\varepsilon(u) = \frac{1}{\delta_\varepsilon^2} \sum_{i,j\in\mathcal{L}\,:|i-j|=1} \varepsilon^2 \left(1 - \frac{|\varepsilon i - \varepsilon j + \delta_\varepsilon(u_i - u_j)|}{\varepsilon}\right)^2 .$$

Hint: use the fact that if $\tilde{u}$ is the piecewise interpolation of u in the triangles of $\varepsilon\mathcal{L}$, then $\nabla\tilde{u}\,\xi = u_{i+\xi} - u_i$, for $\xi \in \{e_1, \frac{1}{2}e_1 \pm \frac{\sqrt{3}}{2}e_2\}$, and the fact that for all $F \in R^{2\times 2}$ and $\xi \in \{e_1, \frac{1}{2}e_1 \pm \frac{\sqrt{3}}{2}e_2\}$ the function $g(\delta) = (1 - |\xi + \delta F\xi|)^2$ has a minimum in $\delta = 0$.[9]

The above linear three-dimensional model for elasticity (1.2.18) reduces to two two-dimensional models, the *plane elasticity model* and the *anti-plane elasticity model* in cylindrical domains, of the form $D \times \mathbb{R}$, where $D \subset \mathbb{R}^2$ represents the cross section of the cylinder, under specific constitutive assumptions.

Plane elasticity: We assume that under applied loads and boundary conditions that do not depend on the variable x_3 and do not have a component in direction e_3, the corresponding displacement be of the form

$$u(x) = (u_1(x_1, x_2), u_2(x_1, x_2), 0)\,.$$

[9]Here we are doing two things at the same time: passage from discrete-to-continuum and linearization. You will see that the dependence on the symmetric gradient in the limit will come out naturally, since the energy, depending only on the relative distances between atoms is frame indifferent.

Under this assumption the energy reduces to the two-dimensional elastic energy

$$\int_D \tilde{\mathbb{C}} e(\tilde{u}) : e(\tilde{u})\, dx\,, \tag{1.2.20}$$

where $\tilde{\mathbb{C}} \in \mathbb{R}^{2\times 2}$ and the $\tilde{u} : D \to \mathbb{R}^2$ is the *plane displacement*.

Anti-plane elasticity: We assume that under applied loads and boundary conditions that do not depend on the variable x_3 and only have the component in direction e_3, the corresponding displacement be of the form

$$u(x) = (0, 0, u_3(x_1, x_2))\,.$$

In this case we obtain the anti-plane energy

$$\int_D C\nabla\hat{u} \cdot \nabla\hat{u}\, dx\,, \tag{1.2.21}$$

where C is a 2×2 matrix and the scalar function $\hat{u} : D \to \mathbb{R}$ is the *vertical displacement*. In the isotropic case we get

$$\int_D \mu|\nabla\hat{u}|^2 dx\,. \tag{1.2.22}$$

1.2.3 Elastic properties of dislocations

We have already noticed that in a crystal with a dislocation, far from the core, the crystal is slightly distorted (i.e., it is locally a small deviation from the perfect crystal, the reference configuration). In this "good" part of the crystal the classical continuum theory for dislocations is developed in the context of linearized elasticity. Actually, the definition of the *core region* is "empirical": it corresponds to the region outside which linear elasticity fits the experiments (see []), it depends on the material and its radius is of the order of the lattice parameter.

The classical computation to evaluate the elastic distortion outside the core is then the one of Volterra for an infinite cylinder (as in Figure 1.20). We consider a displacement u with a jump of $\mathbf{b}$ on the surface Σ, and hence satisfying

$$\mathrm{Curl}\,\nabla u = \mathbf{b} \otimes \mathbf{t}\mathcal{H}^1 \llcorner \mathbf{t}\mathbb{R}\,,$$

and we also require that it satisfies the equilibrium equation

$$\mathrm{Div}(\mathbb{C}\nabla u) = 0 \qquad \text{in } \mathbb{R}^3\,.$$

For the case of an infinite cylinder there are explicit solutions. In the case of a screw dislocation the problem reduces to an anti-plane model with a

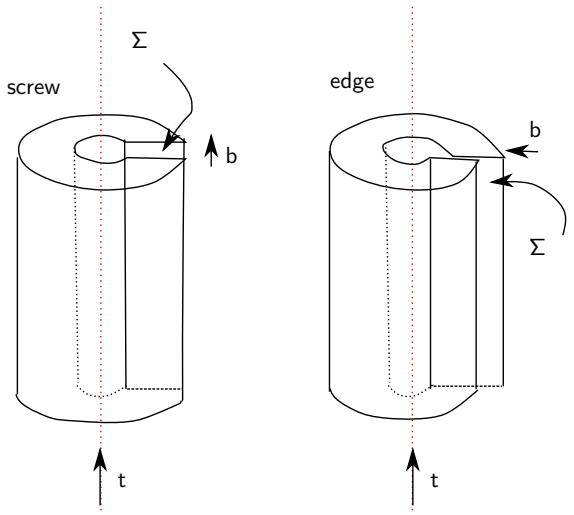

Figure 1.20

scalar vertical displacement that jumps by b. In the isotropic case this is given, in polar coordinates, by

$$u(\rho,\theta) = \frac{b}{2\pi}\theta\,, \tag{1.2.23}$$

and the corresponding elastic strain is

$$\beta^e := \nabla u = \frac{b}{2\pi\rho}\begin{pmatrix} -\sin\theta \\ \cos\theta \end{pmatrix}\,. \tag{1.2.24}$$

Exercise 1.2.2. *Prove that* $\beta = \frac{b}{2\pi\rho}\begin{pmatrix} -\sin\theta \\ \cos\theta \end{pmatrix}$ *satisfies*

$$\mathrm{div}\beta^e = 0 \quad \textit{and} \quad \mathrm{curl}\beta^e = b\delta_0 \qquad \textit{in } \mathbb{R}^2\,,$$

in the sense of distributions.[10]

From (1.2.24) we get

$$\beta^e \sim \frac{1}{\rho}\,. \tag{1.2.25}$$

We will see that this fact is more general. One can prove that if the dislocation line γ is not too irregular, the corresponding elastic strain satisfies $\beta^e(x) \sim \frac{1}{\mathrm{dist}(x,\gamma)}$. This in particular implies that $\beta^e \notin L^2_{\mathrm{loc}}(\mathbb{R}^3)$.

For the explicit anti-plane strain (1.2.24) we can compute the elastic energy in a hollow cylinder of inner radius r and outer radius R, around the

[10]Note that in this case the curl reduces to $\mathrm{curl}\beta = \partial_{x_2}\beta_1 - \partial_{x_1}\beta_2$.

dislocation, which corresponds to compute the L^2 norm of β^e in the set[11] $B_R \setminus B_r \subset \mathbb{R}^2$ and we get

$$\int_{B_R \setminus B_r} |\beta^e|^2 dx = \frac{|b|^2}{4\pi^2} \int_0^{2\pi} \int_r^R \frac{1}{\rho^2} \rho \, d\rho \, d\theta = \frac{|b|^2}{2\pi} \log \frac{R}{r} \,. \tag{1.2.26}$$

Note that this computation provides always a lower bound for the L^2 norm of any field $\beta : B_R \setminus B_r \to \mathbb{R}^2$ satisfying $\mathrm{curl}\beta = b\delta_0$ in the sense of distributions. Indeed this property can be rewritten as

$$\int_{\partial B_\rho} \beta \cdot t \, ds = b \,,$$

where t is the tangent to ∂B_ρ and then, using Jensen inequality, we have

$$\begin{aligned} \int_{B_R \setminus B_r} |\beta|^2 dx &\geq \int_r^R 2\pi\rho \fint_{\partial B_\rho} |\beta \cdot t|^2 \, ds \, d\rho \\ &\geq \int_r^R 2\pi\rho \left| \fint_{\partial B_\rho} \beta \cdot t \, ds \right|^2 d\rho = \frac{|b|^2}{2\pi} \log \frac{R}{r} \,. \end{aligned} \tag{1.2.27}$$

The result is that the linear elastic energy outside the core of the dislocation diverges logarithmically, in the core radius. A similar behavior can be obtained, in plane elasticity, for edge dislocations. This is a general fact; the lack of integrability in L^2 is due to the topological defect. This creates a difficulty in using linear elasticity with an energetic formulation. On the other hand in a discrete description of the interactions between the atoms of the crystal, there is no reason for the dislocation to have such a high energy (indeed the core contains a finite number of interactions). In order to deal with this "inconsistency" in the continuum theory for dislocations there are a number of hybrid models in which different length scales coexist. A continuum variable, as the elastic strain, describes the elastic deformation far from the core and in correspondence to dislocations the problem needs to be regularized with a small parameter that plays the role of the lattice spacing. To simplify matters, there are essentially two main ways, that we will describe more in detail in the sequel, to regularize the problem. These are schematically pictured in the two figures below (see Figure 1.21). In 1) we regularize the elastic energy by removing the core (i.e., an ε-neighborhood $(\gamma)_\varepsilon$ of the dislocation γ) from the elastic energy. We will refer to this approach as the *core radius approach*. This corresponds to considering an energy of the type

$$\int_{\Omega \setminus (\gamma)_\varepsilon} \mathbb{C}\beta\beta dx$$

[11] Here we denote by B_R the ball of radius R centered in 0.

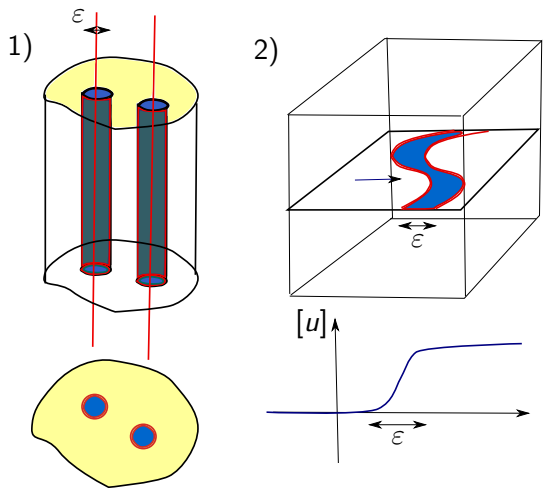

Figure 1.21: 1) The core radius approach. 2) The phase field approach (Nabarro-Peierls)

with the condition $\operatorname{Curl}\beta = \mathbf{b} \otimes \mathbf{t}\mathcal{H}^1 \llcorner \gamma =: \mu$. Alternatively we can consider the energy in the whole of Ω by regularize the elastic strain through a mollification of the measure μ at scale ε, requiring $\operatorname{Curl}\beta = \varphi_\varepsilon \star \mu$.

In 2) the relevant variable is the slip $[u]$ which is regularized by making the transition between two different slips smooth in a layer of length ε. We refer to this model as a *phase field model*.[12]

We will refer to this class of models as *semi-discrete models*, in the sense that, even though continuum models, they represent very well the discrete setting. It can be proved, indeed, in many cases, that the asymptotic behavior of these models gives the same result that could be obtained starting from a genuine discrete description.[13]

[12]The classical reference for this model is the Peierls-Nabarro model (see [8]).
[13]This has been proved rigorously in the case of screw dislocations in [13] and [1] .

Bibliography

[1] R. Alicandro, L. De Luca, A. Garroni, and M. Ponsiglione. Metastability and dynamics of discrete topological singularities in two dimensions: a Γ-convergence approach. *Arch. Ration. Mech. Anal.*, 214(1):269–330, 2014.

[2] L. Ambrosio, N. Fusco, and D. Pallara. *Functions of Bounded Variation and Free Discontinuity Problems*. Mathematical Monographs. Oxford University Press, 2000.

[3] P. G. Ciarlet. *Mathematical elasticity. Vol. I*, volume 20 of *Studies in Mathematics and its Applications*. North-Holland Publishing Co., Amsterdam, 1988. Three-dimensional elasticity.

[4] S. Conti and M. Ortiz. Dislocation microstructures and the effective behavior of single crystals. *Arch. Ration. Mech. Anal.*, 176(1):103–147, 2005.

[5] G. Dal Maso, M. Negri, and D. Percivale. Linearized elasticity as Γ-limit of finite elasticity. *Set-Valued Anal.*, 10(2-3):165–183, 2002. Calculus of variations, nonsmooth analysis and related topics.

[6] L. C. Evans and R. F. Gariepy. *Measure theory and fine properties of functions*. Studies in Advanced Mathematics. CRC Press, Boca Raton, FL, 1992.

[7] M. E. Gurtin. *An introduction to continuum mechanics*, volume 158 of *Mathematics in Science and Engineering*. Academic Press, Inc. [Harcourt Brace Jovanovich, Publishers], New York-London, 1981.

[8] J. P. Hirth and J. Lothe. *Theory of Dislocations*. McGraw-Hill, New York, 1968.

[9] D. Hull and D. J. Bacon. *Introduction to dislocations*. Butterworth-Heinemann, Oxford, UK, 5th edition, 2011.

[10] L. D. Landau and E. M. Lifshitz. *Theory of elasticity*. Course of Theoretical Physics, Vol. 7. Translated by J. B. Sykes and W. H. Reid.

Pergamon Press, London-Paris-Frankfurt; Addison-Wesley Publishing Co., Inc., Reading, Mass., 1959.

[11] J. B. Martin. *Plasticity: Fundamentals and general results*. Princeton Mathematical Series, No. 30. MIT Press, Cambridge, USA, 1975.

[12] J. F. Nye. Some geometrical relations in dislocated crystals. *Acta Metallurgica*, 1:153–162, 1953.

[13] M. Ponsiglione. Elastic energy stored in a crystal induced by screw dislocations: from discrete to continuous. *SIAM J. Math. Anal.*, 39(2):449–469, 2007.